# Computation of Electromagnetic Fields in Large Biological Bodies by an Iterative Moment Method with a Restart Technique

JOHNSON J. H. WANG, SENIOR MEMBER, IEEE, AND JOHN R. DUBBERLEY

*Abstract*—**The computation of EM fields in a large, three-dimensional arbitrarily shaped dielectric or biological body is made practical by a conjugate gradient algorithm with a restart technique. This algorithm allows the operator to run the program for large bodies in a measured and controlled manner. It is clarified that in achieving convergence, a good initial guess plays only a very minor role while the $g^{(n)}$ and $A^{(n)}$ functions are crucial to the convergence in the conjugate gradient algorithm and must be included in the restart.**

## I. Introduction

THE INTERACTION of microwaves with a biological body can have beneficial effects, such as the hyperthermia treatment of a cancerous tumor, and hazardous effects, leading to ailments such as cataracts. In both situations it is essential to know the field intensity inside the biological body under consideration. This is especially important at frequencies in the resonance region, where the field intensity can be rapidly varying and difficult to predict, appearing sometimes as dangerous "hot spots."

Computation of electromagnetic (EM) fields in an arbitrarily shaped dielectric or biological body has been carried out by both direct and iterative methods of moments (MM). In a direct MM, an operation involving a matrix poses a heavy demand on the computer central memory. As a result, the direct MM is limited to objects whose sizes are in the resonance region or smaller. Recently, iterative MM techniques using conjugate gradient (CG) algorithms were developed for two-dimensional problems [1], [2] and expanded to three-dimensional problems [3].

The existence of a certain equivalence between the direct and iterative MM has recently been recognized [3]–[5]. However, the iterative MM has the distinct advantage of being capable of dealing with larger dielectric or biological bodies. For example, on a CDC Cyber 855, the direct MM is limited to an object of 80 cells, or 240 unknowns, each of which can be no greater than, say, half a wavelength (in medium) in linear dimensions. On the other hand, the iterative MM can handle up to 3666 cells, or 11000 unknowns, on this computer.

Manuscript received March 31, 1989; revised June 12, 1989.

The authors are with the Georgia Research Institute, Georgia Institute of Technology, Atlanta, GA 30332.

IEEE Log number 8930811.

In computing large-body problems by an iterative MM, an overriding concern is the huge time and cost of computation. Even when the cost is of no consideration, the operator is likely to be in a state of justifiable apprehension that the computer run lasting days and weeks may at any time be aborted prematurely by operational or system problems.

For large-body problems, the rapidity of convergence is of paramount importance. The question whether an intelligent choice of the initial guess in an iterative MM helps numerical convergence must be addressed, since opinions vary [2], [6]–[8].

In this paper, we present a "restart" technique which allows the operator, or user, of the computer program to monitor and evaluate the numerical process with little sacrifice of computing cost and time. This restart feature enables the operator to minimize the computing cost and to avoid the "crashes" or "disasters" inherent in an extended computer run. We also address the issue of initial guess with specific clarifications.

## II. The Volume Integral Equation Approach

Consider a three-dimensional, arbitrarily shaped dielectric or biological body illuminated by an incident wave $\boldsymbol{E}^i$, which may or may not be a plane wave, as shown in Fig. 1(a). The problem can be formulated by replacing the material body occupying the volume $V$ by an equivalent volume current $\boldsymbol{J}$ as shown in Fig 1(b):

$$\int_V \boldsymbol{J}(\boldsymbol{r}')\cdot\underline{\boldsymbol{G}}_e(\boldsymbol{r},\boldsymbol{r}')\,dv' + D(\boldsymbol{r})\,\boldsymbol{J}(\boldsymbol{r}) = -\boldsymbol{E}^i(\boldsymbol{r}) \qquad \text{for } \boldsymbol{r}\in V \tag{1}$$

where

$$\underline{\boldsymbol{G}}_e = -j\omega\mu_0\left(\underline{\boldsymbol{I}} + \frac{1}{k_0^2}\nabla\nabla\right)g(\boldsymbol{r},\boldsymbol{r}') \tag{2}$$

$$g(\boldsymbol{r},\boldsymbol{r}') = \frac{e^{-jk|\boldsymbol{r}-\boldsymbol{r}'|}}{4\pi|\boldsymbol{r}-\boldsymbol{r}'|} \tag{3}$$

$$\underline{\boldsymbol{I}} = \hat{x}\hat{x} + \hat{y}\hat{y} + \hat{z}\hat{z} \tag{4}$$

$$D(\boldsymbol{r}) = -\frac{\epsilon_r(\boldsymbol{r})+2}{3j\omega[\epsilon(\boldsymbol{r})-\epsilon_0]}. \tag{5}$$

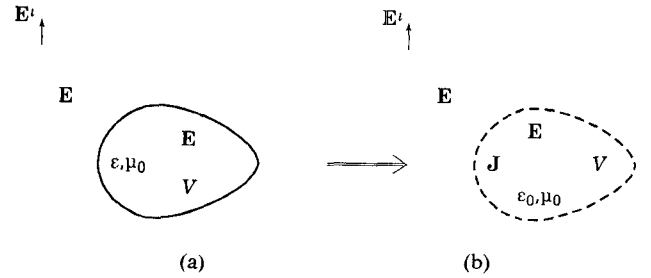


Fig. 1. (a) Dielectric body illuminated by $E^i$. (b) Replacing the dielectric body with a volume current $J$.

Here $\epsilon$ is the permittivity of the medium, $\epsilon_r$ is the relative permittivity, and $\epsilon = \epsilon_r \epsilon_0$. $r$ and $r'$ denote the position vectors at the field and source points respectively. $k_0^2 = \omega^2 \epsilon_0 \mu_0$ and the hat "^" denotes a unit vector. $f$ denotes a principal-value integration with an infinitesimal sphere centered at $r = r'$ extracted.

Equation (1) can be written in the following form:

$$\int_V \boldsymbol{J}(\boldsymbol{r}') \cdot \underline{\boldsymbol{K}}(\boldsymbol{r}, \boldsymbol{r}')\, dv' = -\boldsymbol{E}^i(\boldsymbol{r}) \qquad \text{for } \boldsymbol{r} \in V \tag{6}$$

or, in general,

$$\int_V \boldsymbol{x}(\boldsymbol{r}') \cdot \underline{\boldsymbol{K}}(\boldsymbol{r}, \boldsymbol{r}')\, dv' = \boldsymbol{y}(\boldsymbol{r}) \qquad \text{for } \boldsymbol{r} \in V. \tag{7}$$

Solution of the integral equation begins by discretizing the volume $V$ into $L$ cubic volume cells $V_1, V_2, \cdots, V_L$, generally of different cell sizes. This is carried out by expanding $J$ as

$$\boldsymbol{J}(\boldsymbol{r}) = \sum_{l=1}^{L} \sum_{k=1}^{3} J_l^k \boldsymbol{B}_l^k(\boldsymbol{r}) \tag{8}$$

where

$$\boldsymbol{B}_l^k(\boldsymbol{r}) = \hat{u}_k B_l^k(\boldsymbol{r}) = \hat{u}_k P_l(\boldsymbol{r}) \tag{9}$$

$$P_l(\boldsymbol{r}) = 1, \qquad \boldsymbol{r} \in V_l$$
$$= 0, \qquad \text{elsewhere.} \tag{10}$$

Here $\hat{u}_k$ are unit vectors, being $\hat{x}$, $\hat{y}$, and $\hat{z}$ for $k = 1$, 2, and 3 respectively in rectangular coordinates.

In a direct MM, weighting functions are chosen as

$$\boldsymbol{W}_m^k(\boldsymbol{r}) = \delta(\boldsymbol{r} - \boldsymbol{r}_m)\hat{u}_k. \tag{11}$$

By performing a symmetric product with $W_m^k$ on (1) and with $J$ discretized by (8), for $m = 1, \cdots, L$ and $k = 1$, 2, 3, one obtains $3L$ linear equations, or a $3L \times (3L + 1)$ matrix equation, which can be solved for the unknown $J_l^k$.

## III. Iterative Conjugate Gradient Algorithm with Restart Feature

A three-dimensional iterative conjugate gradient (CG) algorithm for solving (6) or (7) with the unknown equivalent volume current $J$ discretized according to (8) has been successfully developed by the present authors [3]. This algorithm was applied to large dielectric and biological bodies including a 423-cell human body. The computation begins with a given initial guess $x^{(0)}(r)$ and terminates when either a preset accuracy criterion or the maximum number of iterations is reached. The error criterion is the commonly adopted "normalized integrated square error," defined as

$$ERRN = \frac{ERR^{(N)}}{\int_V |\boldsymbol{x}^0(\boldsymbol{r}')|^2\, dv'} \tag{12}$$

where $ERR^{(N)}$ is the "integrated square error," defined as

$$ERR^{(N)} = \int_V \left| \boldsymbol{y}(\boldsymbol{r}) - \int_V \boldsymbol{x}^{(N)}(\boldsymbol{r}') \cdot \underline{\boldsymbol{K}}(\boldsymbol{r}, \boldsymbol{r}')\, dv' \right|^2 dv. \tag{13}$$

For the continuous integral equation (7), $ERR^{(N)}$ is zero if and only if $x^{(N)}(r)$, the solution after $N$ iterations, satisfies (7) at every point $r$ in $V$. However, since it is the discretized integral equation that is being solved, $ERR^{(N)}$ would be zero if $x^{(N)}(r)$ satisfied (7) in a least-squares sense.

To run an iterative algorithm, one presets either $ERR^{(N)}$ for the desired accuracy or a maximum number of iteration $N_{\max}$, or both, so that the computational process will terminate automatically. An agonizing dilemma for the operator in running large-body problems is to choose $ERR^{(N)}$ and $N_{\max}$ based on a projected trade-off between desired accuracy and computational cost. Since the course of the actual iterative process is difficult to predict, a computer run often terminates prematurely or continues for many more unnecessary iterations. Thus it is desirable to have a pause in the computer run after a certain number of iterations and allow the operator to make an evaluation and adjustment for the computational process.

The idea of pause and restart, or a similar procedure, for an iterative algorithm had been explored by Sultan and Mittra [7] and Davey and Montgomery [8]. In their methods, $n$ iterations were first carried out, leading to a resulting $x^{(n)}(r)$. Then a fresh new start with $x^{(n)}(r)$ as the initial guess is made. (The restart of Sultan and Mittra is based on the same principle, but is slightly different in details). Their basic rationale is that a good initial guess should lead to the "correct" result in fewer iterations than a poor initial guess.

We have observed that, as far as the rate of convergence is concerned, the knowledge and assignment of the $g^{(n)}$ vector and coefficient $A^{(n)}$ are much more important than the selection of a good initial guess. We have developed a new CG algorithm with a restart feature as shown in Fig. 2. The iterative process begins with an initial guess $x^{(0)}$ chosen by the operator. However, the iterative process will pause and dump $g^{(n)}$, $A^{(n)}$, and $x^{(n)}$ into a tape file after a preset $N_{\max}$ or $ERR^{(n)}$ is reached. The operator then examines the data to decide what new $N_{\max}$ and $ERR^{(n)}$ should be chosen for the next restart run. At the beginning of the restart, the computer reads from a tape file $g^{(n)}$, $A^{(n)}$, and $x^{(n)}$; consequently the restart is in effect a perfect continuation of the process from the $n$th iteration of the regular CG algorithm in [3]. Thus the restart CG algorithm takes advantage not only of a better initial guess, but also of the desired direction and magnitude of the correction learned in a prior CG run.

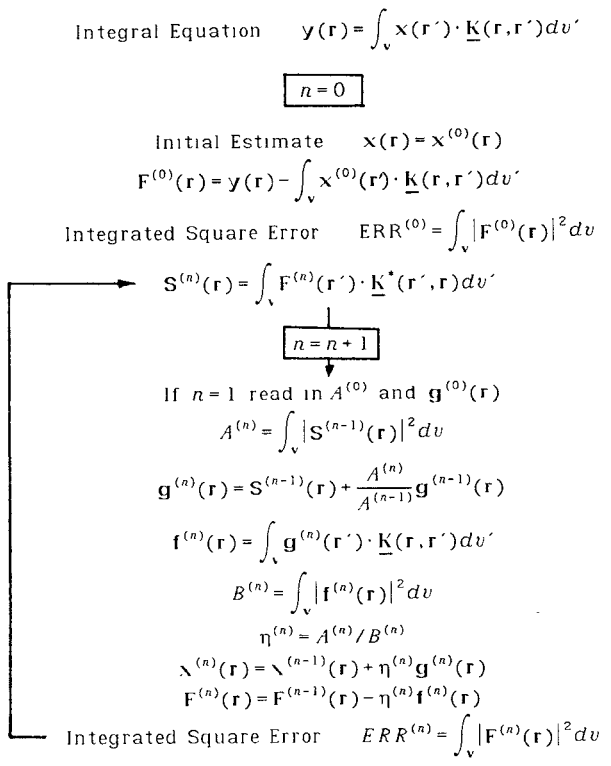


Fig. 2. A 3-D conjugate gradient algorithm with restart feature.

## IV. The Restart Feature and the Effects of Initial Guess

The present CG algorithm with a restart feature allows the operator to pause and adjust an iterative run to fine-tune for the desired accuracy within his budget for computational time and cost. It will also reduce the chance of being aborted prematurely, as frequently happens in runs lasting days or weeks. The price for this feature is mainly an additional central memory allocated for $(6L+1)$ complex numbers ($3L$ each for $\boldsymbol{x}^{(0)}$ and $\boldsymbol{g}^{(0)}$ and 1 for $A^{(0)}$), where $L$ is the number of cells in (8). This results in a reduction by about 12 percent in the size of the biological object (or the number of unknowns) that can be solved on a computer. There is also a slight increase in execution time for reading the input data for $\boldsymbol{x}^{(0)}$, $\boldsymbol{g}^{(0)}$, and $A^{(0)}$ at the beginning of the run and a similar amount of time to store these three variables.

Although the restart CG algorithm was developed primarily for large-body problems, it is easier to first demonstrate the method and its advantages on smaller and simpler objects. Fig. 3 shows the front, side, and bottom views of a dielectric block discretized into 24 cubic cells. The relative permittivity $\epsilon_r$ of the block is $71.7-j6.53$. A plane wave at 2450 MHz with $z$ polarization propagates in the direction of the $x$ axis.

Fig. 4 shows the total electric field at the center of cell no. 22, which is at $x=0$, $y=0.482$ cm, and $z=0$. Four sets of computational results are displayed in this figure. The bottom straight line is the result of a direct MM point-matching solution. Three iterative computations were made, all of which converge to the direct MM result within

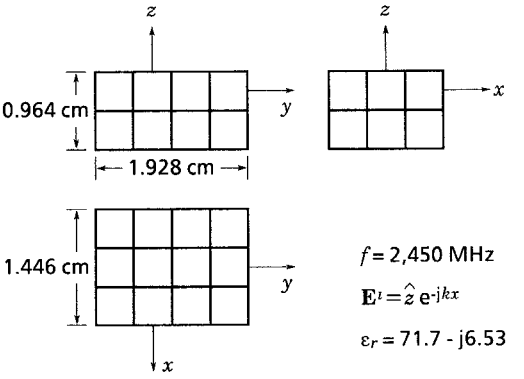


Fig. 3. A dielectric block discretized into 24 cubic cells.

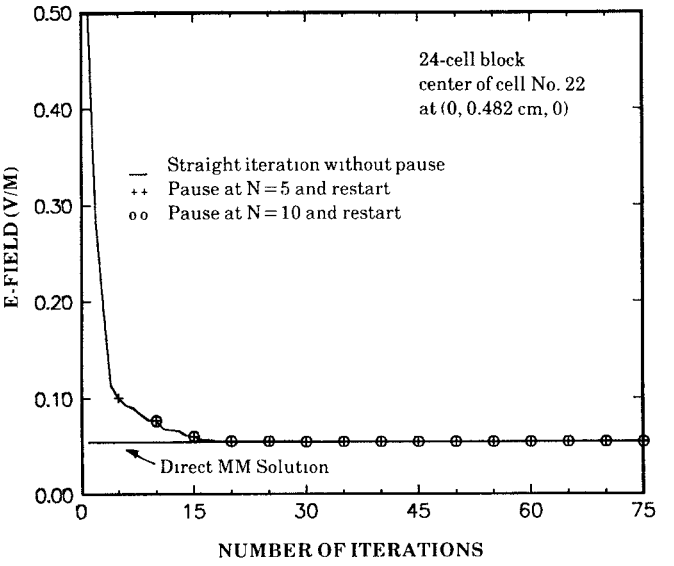


Fig. 4. Computed fields in dielectric block showing successful pause and restart in an iterative computation.

six significant figures, indicating an equivalence between the present iterative MM algorithm and a direct MM with point matching.

Among the three iterative runs, one is a continuous procedure that terminates after the preset 75 iterations, the second one pauses after the fifth iteration and then resumes, and the third one pauses after the tenth iteration and then resumes. As can be seen, the continuity of the iterative process is not affected by the pauses. Also, convergence is achieved after the 20th iteration. The pauses allow the operator to evaluate and control the progress and terminate the computation in a measured and controlled manner.

A global view of the convergence phenomenon is shown in Fig. 5, in which the simple line is for a straight iterative computation, and the line with crosses is for a restart run with $\boldsymbol{x}^{(0)}$, $\boldsymbol{g}^{(0)}$, and $A^{(0)}$ read from $\boldsymbol{x}^{(20)}$, $\boldsymbol{g}^{(20)}$, and $A^{(20)}$ from a paused prior run. As can be seen, *ERRN* in the restart run is 20 iterations ahead of that of a straight run, indicating that the advantage of having a better $\boldsymbol{x}^{(0)}$, $\boldsymbol{g}^{(0)}$, and $A^{(0)}$ in restart is maintained until *ERRN* drops to below $10^{-15}$, where numerical round-off errors introduced in earlier input and output at pauses begin to take effect.

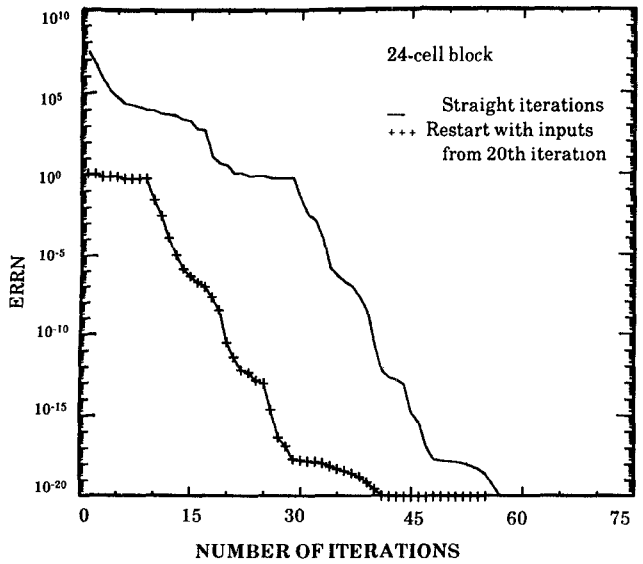


Fig. 5. Comparison of the rate of convergence between straight and restart iterations.

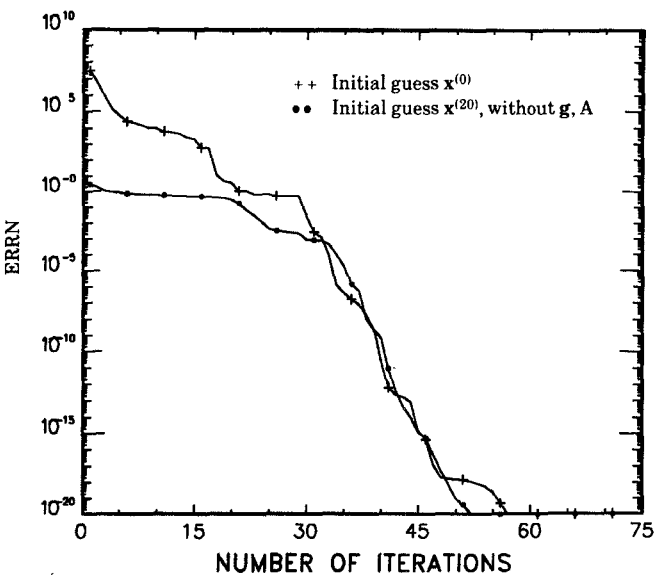


Fig. 6. Comparison showing poor rate of convergence in a restart that reads in initial guess only.

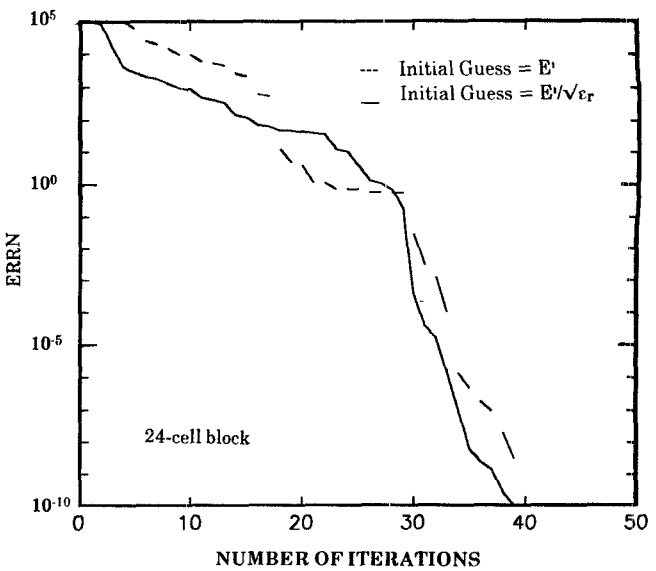


Fig. 7. Rate of convergence little affected by initial guesses.

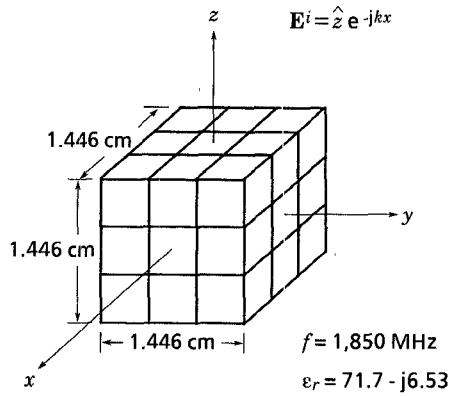


Fig. 8. A dielectric cube discretized into 27 cubic cells.

As a comparison between the costs of these two runs, we noted that it took 248.7 s on a CDC Cyber 855 for the straight 75 iterations, while it took 252.4 s for the restart procedure including 20+55, or 75, total iterations. The difference is truly minimal. When the restart is carried out with the informed initial guess $x^{(20)}$ only, without $g^{(20)}$ and $A^{(20)}$, there is little advantage in the rate of convergence exhibited by this better initial guess. This is illustrated in Fig. 6, which can be compared with Fig. 5 for the effects of restart with and without inputting $g^{(20)}$ and $A^{(20)}$. (In both restarts $x^{(20)}$ is read in as $x^{(0)}$ from input files.)

As an additional comparison, Fig. 7 shows a comparison for the block problem of Fig. 3 between two different initial guesses in a straight iterative run without pause. The initial guess of $E^i/\sqrt{\epsilon_r}$, or 0.118 in magnitude, is much closer to the correct answer (0.0553 in cell no. 22) than the initial guess of $E^i$, 1.0 in magnitude. However, this significant advantage in initial guess vanishes steadily and was totally lost after the 18th iteration and regained after the 29th iteration. This again demonstrates that the initial guess $x^{(0)}$ plays a truly minor role in the rate of convergence in CG compared with $g^{(0)}$ and $A^{(0)}$.

Thus in searching for a solution by iterative means in a three-dimensional problem, it is much more important to know the direction in which to go than to be near the correct location (result), even though a good initial guess per se is a definite initial advantage.

Let us examine another case in Fig. 8, a cubic dielectric body discretized into 27 cubic cells. Fig. 9 shows the total electric field at the center of the cube in Fig. 8 computed by a direct MM and three iterative procedures, two of which pause at $n=10$ and $n=20$ respectively and restart, and one without pause. Fig. 10 shows a comparison of the rates of convergence for the cube case between a straight iterative CG computation and a restart computation with $x^{(0)}$, $g^{(0)}$, and $A^{(0)}$ read from $x^{(15)}$, $g^{(15)}$, and $A^{(15)}$ from a previous run. Figs. 9 and 10 for the cube case exhibit characteristics similar to those seen in Figs. 4 and 5 for the

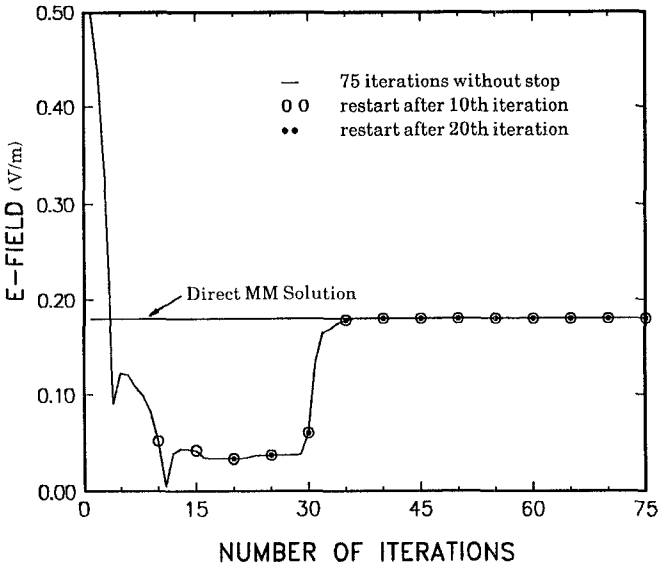


Fig. 9. Computed fields in dielectric cube showing successful pause and restart in an iterative computation.

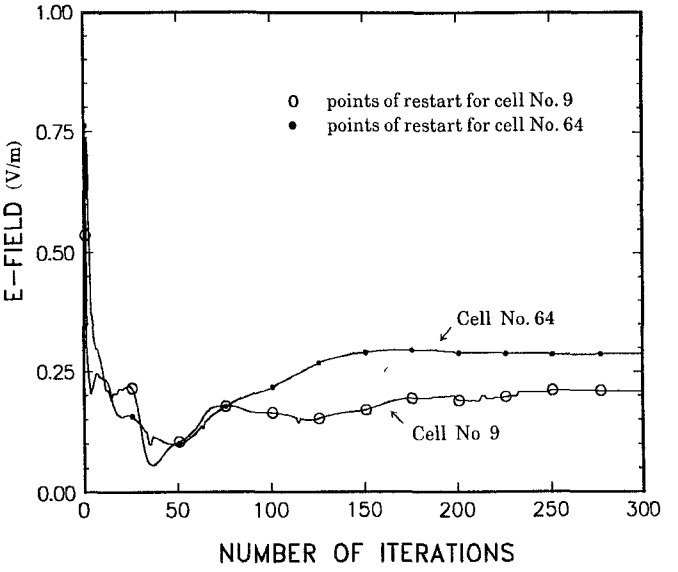


Fig. 11. Convergence of field in cells 9 and 63 for the 423-cell human body.

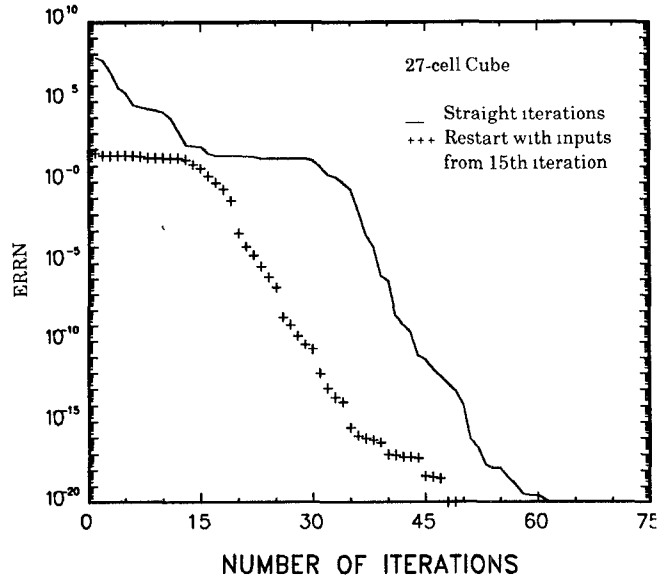


Fig. 10. Comparison of the rate of convergence between straight and restart iterations.

block case, and support the conclusions drawn earlier on the role of the initial guess.

The restart CG algorithm was applied to the case of the large 423-cell (1269-unknown) human body described in [3]. The runs were paused and restarted after every 25 iterations. The choice of 25 iterations between pauses was made after our first 50-iteration run was aborted by the system operator after a few days on the Cyber. The normalized integrated square error *ERRN* is observed to decrease monotonically with the total number of iterations *N*. However, instead of the staircase feature seen in Figs. 5, 6, and 10 for smaller objects, the decrease of *ERRN* is more gradual in this case. This may be due to round-off errors that are more prominent in large-body computations.

Fig. 11 shows the convergence of electric field intensity in cells 9 and 63 as the total number of iterations *N* increases. The dots and circles mark all the points of pause and restart, which occur after every 25 iterations. The tiny jitter of fields in cell no. 9 is probably related to the resonance phenomena in the head region, where cell no. 9 is located. Let us compare Fig. 11 with the same case in [3], in which 75 straight iterations were run according to a preset maximum number of iterations (chosen to be 75). This choice of 75 iterations was a trade-off between the desired accuracy, computational cost, and possible operator or system drop that may happen to extremely long runs lasting for weeks. In the present runs leading to Fig. 11, we paused and restarted as needed, to be sure of obtaining the desired data in an optimum number of iterations in a controlled and organized manner.

## V. Conclusions

A restart conjugate gradient algorithm for a three-dimensional arbitrarily shaped dielectric body has been successfully developed. The restart method breaks a long iterative run into short runs so that no premature aborting will take place and that the operator can control the iterative process in a measured, and thus cost-effective, manner. In developing this restart algorithm, the ambiguity regarding the effect of initial guess is clarified. We established that the $g$ and $A$ functions, rather than the initial guess, are crucial to the rate of convergence.

## References

[1] P. M. van den Berg, A. T. de Hoop, A. Segal, and N. Praagman, "A computational model of the electromagnetic heating of biological tissue with application to hyperthermic cancer therapy," *IEEE Trans. Biomed. Eng.*, vol. BME-30, pp. 797–805, Dec. 1983.

[2] P. M. van den Berg, "Iterative computational techniques in scattering based upon the integrated square error criterion," *IEEE Trans. Antennas Propagat.*, vol. AP-32, pp. 1063–1071, Oct. 1984.

[3] J. J. H. Wang and J. R. Dubberley, "Computation of fields in an arbitrarily shaped heterogeneous dielectric or biological body by an

iterative conjugate gradient method," *IEEE Trans. Microwave Theory Tech.*, vol. 37, pp. 1119–1125, July 1989.
[4] J. J. H. Wang, "Generalization and interpretation of the moment method in electromagnetics," *IEEE Trans. Microwave Theory Tech.*, to be published.
[5] S. L. Ray and A. F. Peterson, "Error and convergence in numerical implementations of the conjugate gradient method," *IEEE Trans. Antennas Propagat.*, vol. 36, pp. 1824–1827, Dec. 1988.
[6] A. F. Peterson and R. Mittra, "Convergence of the conjugate gradient method when applied to matrix equations representing electromagnetic scattering problems," *IEEE Trans. Antennas Propagat.*, vol. AP-34, pp. 1447–1454, Dec. 1986.
[7] M. F. Sultan and R. Mittra, "An iterative moment method for analyzing the electromagnetic field distribution inside inhomogeneous lossy dielectric objects," *IEEE Trans. Microwave Theory Tech.*, vol. MTT-33, pp. 163–168, Feb. 1985.
[8] J. P. Montgomery and K. R. Davey, "The solution of planar periodic structures using iterative methods," *Electromagnetics*, vol. 5, nos. 2–3, pp. 209–235, 1985.

✠

**Johnson J. H. Wang** (M'68–SM'79) was born in Hunan, China, on October 24, 1938. He received the B.S.E.E. degree from National Taiwan University, the M.S. degree from Florida State University, Tallahassee, FL and the Ph.D. degree from Ohio State University, Columbus, in 1962, 1965, and 1968, respectively.

From 1968 to 1975, he worked at a number of industrial firms. In 1975, he joined the Georgia Institute of Technology, Atlanta, GA. His research interests include antennas, bioelectromagnetics, radiation and scattering measurements, microwave imaging, and numerical methods in solving electromagnetic problems.

✠

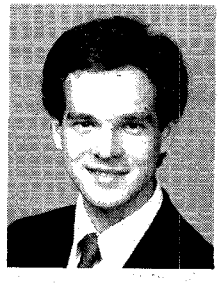

**John R. Dubberley** was born in Opelika, AL, on May 28, 1966. He received the B.E.E. degree from the Georgia Institute of Technology, Atlanta, GA, in June 1988, and is currently enrolled in the Ph.D. program in the School of Electrical Engineering there. He has worked at Georgia Tech Research Institute of Georgia Tech, first as a co-op student and then as a Graduate Research Assistant, on a wide range of electromagnetic problems, including near-field measurements and numerical analyses.